JNeurosci
THE JOURNAL OF NEUROSCIENCE

Research Articles: Systems/Circuits

Corticosterone Production during Repeated Social Defeat Causes Monocyte Mobilization from the Bone Marrow, Glucocorticoid Resistance and Neurovascular Adhesion Molecule Expression

Anzela Niraula[1,2], Yufen Wang[3], Jonathan P. Godbout[1,2,3,4] and John F. Sheridan[1,2,3]

[1]*Division of Biosciences, The Ohio State University*
[2]*Department of Neuroscience, The Ohio State University*
[3]*Institute for Behavioral Medicine Research, The Ohio State University*
[4]*Center for Brain and Spinal Cord Repair, The Ohio State University*

DOI: 10.1523/JNEUROSCI.2568-17.2018

Received: 7 September 2017

Revised: 9 January 2018

Accepted: 17 January 2018

Published: 30 January 2018

Author contributions: A.N., J.P.G., and J.F.S. designed research; A.N. and Y.W. performed research; A.N. analyzed data; A.N. and J.P.G. wrote the paper; J.P.G. and J.F.S. contributed unpublished reagents/analytic tools.

Conflict of Interest: The authors declare no competing financial interests.

This study was supported by National Institute of Health (NIMH) grants R01-MH-093473 and R01-MH097243 to J.F.S. and National Institute of Aging grant R01-AG033028 to J.P.G. We thank Rahul Gupta for his technical assistance.

Corresponding author: John F. Sheridan (Sheridan.1@osu.edu)

Cite as: J. Neurosci ; 10.1523/JNEUROSCI.2568-17.2018

Corticosterone Production during Repeated Social Defeat Causes Monocyte Mobilization from the Bone Marrow, Glucocorticoid Resistance and Neurovascular Adhesion Molecule Expression

Abbreviated title: Corticosterone induced monocyte release with RSD

Anzela Niraula[1,2], Yufen Wang[3], Jonathan P. Godbout[1,2,3,4], and John F. Sheridan[1,2,3,5]

[1] Division of Biosciences, The Ohio State University
[2] Department of Neuroscience, The Ohio State University
[3] Institute for Behavioral Medicine Research, The Ohio State University
[4] Center for Brain and Spinal Cord Repair, The Ohio State University

[5] Corresponding author: John F. Sheridan (Sheridan.1@osu.edu)

Keywords: stress, corticosterone, neuroinflammation, neuroimmune, monocytes, anxiety

This study was supported by National Institute of Health (NIMH) grants R01-MH-093473 and R01-MH097243 to J.F.S. and National Institute of Aging grant R01-AG033028 to J.P.G. We thank Rahul Gupta for his technical assistance. The authors declare no competing financial interests.

Number of words in title = 20
Number of words in abstract = 228
Number of words in significance statement = 125
Number of words in introduction = 745
Number of words in discussion = 1495

Abstract

Repeated social defeat (RSD) stress promotes the release of bone marrow-derived monocytes into circulation that are recruited to the brain, where they augment neuroinflammation and cause prolonged anxiety-like behavior. Physiological stress activates the sympathetic nervous system (SNS) and hypothalamic-pituitary-adrenal gland (HPA) axis, and both of these systems play a role in the physiological, immunological, and behavioral responses to stress. The purpose of this study was to delineate the role of HPA activation and corticosterone production in the immunological responses to stress in male C57/BL6 mice. Here, surgical (adrenalectomy) and pharmacological (metyrapone) interventions were used to abrogate corticosterone signaling during stress. We report that both adrenalectomy and metyrapone attenuated the stress-induced release of monocytes into circulation. Neither intervention altered the production of monocytes during stress, but both interventions enhanced retention of these cells in the bone marrow. Consistent with this observation, adrenalectomy and metyrapone also prevented the stress-induced reduction of a key retention factor, CXCL12, in the bone marrow. Corticosterone depletion with metyrapone also abrogated the stress-induced glucocorticoid resistance of myeloid cells. In the brain, these corticosterone-associated interventions attenuated stress-induced microglial remodeling, neurovascular expression of the adhesion molecule ICAM-1, prevented monocyte accumulation and neuroinflammatory signaling. Overall, these results indicate that HPA activation and corticosterone production during repeated social defeat stress are critical for monocyte release into circulation, glucocorticoid resistance of myeloid cells, and enhanced neurovascular cell adhesion molecule expression.

55 **Significance statement**

56

57 Recent studies of stress have identified the presence of monocytes that show an exaggerated
58 inflammatory response to immune challenge and are resistant to the suppressive effects of
59 glucocorticoids. Increased presence of these proinflammatory monocytes has been implicated in
60 neuropsychiatric symptoms and the development of chronic cardiovascular, autoimmune and
61 metabolic disorders. In the current study, we show novel evidence that corticosterone produced
62 during stress enhances the release of proinflammatory monocytes from the bone marrow into
63 circulation, augments their recruitment to the brain and the induction of a neuroinflammatory
64 profile. Overproduction of corticosterone during stress is also the direct cause of glucocorticoid
65 resistance, a key phenotype in individuals exposed to chronic stress. Inhibiting excess
66 corticosterone production attenuates these inflammatory responses to stress.

67

68

69

70

Introduction

Psychological stress contributes to the development and exacerbation of anxiety-like disorders (Kendler et al. 1999, Pasquali 2012). Activation of the sympathetic system (SNS) and the hypothalamic-pituitary-adrenal (HPA) axis regulates the immunological and behavioral responses to stress. For instance, HPA activation during stress corresponds with the release of glucocorticoids from the adrenal cortex. Glucocorticoids regulate glucose and energy mobilization, and immune functions in response to stress (Sapolsky et al. 2000). Chronic stress, however, leads to glucocorticoid resistance and enhanced inflammatory signaling in humans and rodents (Pace et al. 2006, Cohen et al. 2012). For instance, low socioeconomic status and prolonged caregiving stress in humans are associated with a "transcriptional fingerprint", characterized by enhanced expression of proinflammatory signals in peripheral monocytes and resistance to the suppressive effects of glucocorticoids (Miller et al. 2008, Miller et al. 2014). Individuals exposed to chronic stress show high levels of circulating IL-6, which is a strong indicator of stress-induced psychiatric and cardiovascular disorders (Maes et al. 1999, Maes et al. 2012). Importantly, IL-6 is an acute phase protein regulated by the HPA axis (Zhou et al. 1993). Thus, over-activation of the HPA axis, along with a blunted response to corticosterone, may lead to unchecked inflammatory responses that are associated with stress-induced neuropsychiatric, metabolic and cardiovascular diseases (Walker 2007, Sorrells et al. 2009, Marin et al. 2011).

The clinical features of chronic stress (e.g., glucocorticoid resistance, enhanced proinflammatory profile, and elevated plasma IL-6) are recapitulated in the repeated social defeat model (RSD) of stress in mice (Wohleb et al. 2014, Reader et al. 2015). RSD increases neuronal and microglial activation, endothelial cell adhesion molecule expression, production and release of monocytes into circulation, and recruitment to tissues, including the brain (McKim et al.

2017). Increased presence of circulating monocytes has been reported in stressed individuals, and monocyte accumulation in the brain vasculature was reported in depressed suicide victims (Heidt et al. 2014, Torres-Platas et al. 2014). We have identified monocytes in the RSD brain as the pro-inflammatory ($CCR2^{+}Ly6C^{hi}$) type that propagates IL-1-receptor signaling at the brain vascular endothelium, causing prolonged anxiety-like behavior (McKim et al. 2017) and long-lasting "stress sensitization" to subsequent stressors (Wohleb et al. 2014, McKim et al. 2015). Other recent studies with social defeat in mice show that accumulation of pro-inflammatory monocytes in the neurovasculature triggers neuropsychiatric complications (Menard et al. 2017). Therefore, mobilization of inflammatory monocytes from the bone marrow represents an important mechanism for CNS signaling to the immune system during stress (Weber et al. 2017).

Exposure to RSD also promotes the induction of glucocorticoid resistance in myeloid cells. For instance, myeloid cells from the spleen of mice exposed to RSD are resistant to the anti-inflammatory effects of glucocorticoids (e.g. enhanced IL-6 production following LPS and sustained viability despite high corticosterone exposure) (Avitsur et al. 2001, Stark et al. 2001). This glucocorticoid insensitive phenotype of splenocytes following RSD is significant because it is also present in peripheral monocytes from individuals suffering from chronic stress (Miller et al. 2002, Miller et al. 2008). Furthermore, monocytes that accumulated in the brain during RSD displayed an mRNA profile consistent with glucocorticoid resistance, i.e. reduced glucocorticoid receptor and increased IL-1β expression (McKim et al. 2017). In addition, stress-induced glucocorticoid resistance was associated with elevated inflammatory response to subsequent innate immune challenge (Quan et al. 2001, Wohleb et al. 2012). Glucocorticoid resistance with RSD was associated with a failure of the glucocorticoid receptor in myeloid cells to translocate into the nucleus (Quan et al. 2003).

Both HPA and SNS pathways communicate with the immune system in response to stress. For instance, beta-adrenergic intervention and benzodiazepines prevented the RSD-induced activation of threat appraisal and all downstream changes in the brain and the periphery (Wohleb et al. 2011, Hanke et al. 2012, Ramirez et al. 2016). Notably, inhibition of threat appraisal during RSD prevented both HPA and SNS activation. Therefore, the purpose of this study was to delineate the role of corticosterone in the peripheral immune response to stress. This is important because corticosterone, generally suppresses inflammatory signaling, but also has pleiotropic effects (Sorrells et al. 2009). Furthermore, the role of corticosterone on monocyte production, release and tissue recruitment during stress is unknown. In the current study, we show for the first time that corticosterone production during RSD promoted mobilization of monocytes from the bone marrow into circulation. Moreover, we provide novel evidence that corticosterone caused glucocorticoid resistance in myeloid cells, and enhanced cell adhesion molecule expression and inflammatory mediators in the brain during RSD.

132 **Materials and methods**

133

134 ***Mice:*** Male C57BL/6 mice (6-8 week old) and CD-1 mice (12 month old, retired breeders) were
135 purchased from Charles River Breeding Laboratories (Wilmington, MA). Adrenalectomized and
136 sham C57BL/6 mice (6-8 week old) were purchased from Jackson Laboratories, Bar Harbor,
137 ME. All adrenalectomized mice were provided with supplemental corticosterone (25 µg/mL) in
138 drinking water until sacrifice (Lehmann et al. 2013). Next, CXCL12-DsRed mice were
139 generously provided by Sean J. Morrison at University of Texas Southwestern Medical Center.
140 All experimental mice were housed in cohorts of three, while CD-1 mice were individually
141 housed. Mice were kept in 11.5 x 7.5 x 6 inch polypropylene cages, and were maintained at 21°
142 under a 12 hour light/dark cycle with access to food and water *ad libitum* at the animal housing
143 facility at The Ohio State University. All mice were allowed to acclimate for 7-10 days before
144 initiation of any experimental procedure. All procedures were in accordance with the NIH
145 Guidelines for the Care and Use of Laboratory Animals, and performed with approval from the
146 The Ohio State University Institutional Animal Care and Use Committee.

147

148 ***Repeated Social Defeat:*** The repeated social defeat model of stress involves eliciting a flight or
149 fight in resident mice in response to an aggressive intruder. In contrast to pair fighting paradigms
150 of stress, RSD adds a key social component that includes psychological stress caused due to
151 disruption of the social hierarchy within an established cohort of resident mice. In the current
152 study, we performed RSD as previously reported (Avitsur et al. 2001, Wohleb et al. 2013). In
153 brief, a CD-1 aggressor was introduced into the cage of an established cohort (3 mice) of
154 C57BL/6 mice for 2 hours (17:00 to 19:00 h) daily for 6 consecutive nights. If the intruder

mouse did not attack in the first 5 minutes, it was replaced by a new intruder. Different intruder mice were used on consecutive days. During each episode of stress, resident mice were monitored for submissive behaviors including, crouching, fleeing and upright posture. At the end of the 2 h period, the intruder mice were returned to their original cages, and the resident mice were left undisturbed until the next episode of stress the following day. The health status of the mice was carefully examined throughout the experiment. In the event of an injury, mice were removed from the experiment. Consistent with our previous studies, less than 5% of the mice met early removal criteria. The control mice were left undisturbed in their home cages during the study.

Experimental protocols

ADX intervention and stress: Male C57BL/6 mice were subjected to sham or adrenalectomy (ADX) surgery at Jackson Laboratories. Mice were shipped to OSU and allowed 7 days to recover. All adrenalectomized mice were provided with supplemental corticosterone (25 µg/mL) in drinking water until sacrifice (Lehmann et al. 2013). Under homeostatic conditions, corticosterone production follows a circadian oscillatory pattern, i.e. sustained increases during active phase and reduction during passive phase. This oscillatory production of corticosterone is necessary in maintaining the physiological functions (e.g. homeostatic ACTH levels) but not enough to elicit a stress response (Jacobson et al. 1988, Dhabhar et al. 2012). Because adrenalectomized mice are unable to produce corticosterone, the supplemental corticosterone in drinking water is necessary to maintain the circadian rhythmicity of corticosterone in these mice.

Next, mice were exposed to 6 cycles of repeated social defeat (Stress). Plasma for corticosterone was collected via submandibular bleeds immediately after stress (3 experiments, n=3-4 per experiment). In addition, bone marrow, blood, spleen, and brain (2 experiments, n=3-4 per experiment) were collected 14 h after the last cycle of stress. IL-6 protein levels were determined in plasma (2 experiments, n=3-4 per experiment). Percentage of monocytes and granulocytes (2 experiments, n=3-4 per experiment) were determined in the blood and bone marrow, and CXCL12 mRNA levels (2 experiments, n=3-4 per experiment) were also determined in the bone marrow. For brain mRNA levels, a 1 mm coronal section from the brain (approximately -0.34 mm to -1.34 mm Bregma) was collected (2 experiments, n=3-4 per experiment) and the rest of the brain was used to collect CD11b+ cells for flow cytometry (2 experiments, n=3-4 per experiment). In a separate study, mice were treated as above, and were perfused and paraformaldehyde-fixed. ICAM-1 expression was determined by immunohistochemistry (1 experiment, n=3-4).

CXCL12 reporter and stress: Male CXCL12-DsRed mice were exposed to control or repeated social defeat (Stress). Mice were perfused, paraformaldehyde-fixed, and bone marrow was collected to evaluate RFP expression (1 experiment, n=3)

Metyrapone intervention and stress: Male C57BL/6 mice were injected intraperitoneally daily with either vehicle (water) or 100 mg/kg metyrapone (Enzo Life Sciences, Farmingdale, NY; Catalog# BML-EI256) 30 minutes prior to control or repeated social defeat (Stress). Plasma for corticosterone was collected via submandibular bleed immediately after stress (2 experiments, n=3-4 per experiment). In addition, bone marrow, blood, spleen, and brain (2 experiments, n=3-4 per experiment) were collected 14 h after the last cycle of stress. IL-6 protein levels were determined in plasma (1 experiment, n=3-4). Percentage of monocytes and

granulocytes determined in the bone marrow and blood (2 experiments, n=3-4 per experiment). CXCL12 mRNA levels were determined in the bone marrow (1 experiment, n=3-4). For mRNA analysis in the brain, a 1 mm coronal section from the brain (approximately -0.34 mm to -1.34 mm Bregma) was collected (2 experiments, n=3-4 per experiment), and the rest of the brain was used to collect $CD11b^+$ cells for flow cytometry. In a separate study mice were treated as above and mice were perfused and paraformaldehyde-fixed. ΔFosB, Iba-1 and ICAM-1 expression were determined by immunohistochemistry (1 experiment, n=3-4). In a final study, mice were treated as above with MTP and exposed to stress. The spleen was collected 14 h after the last cycle of stress. Splenocytes were cultured *ex vivo* with LPS and treated with increasing doses of corticosterone. Cell survival and supernatant IL-6 levels were determined (2 experiments, n=3-4 per experiment).

Isolation of CD11b$^+$ cells from the brain: $CD11b^+$ cells were enriched by Percoll isolation as described previously (Wohleb et al. 2013). At 14 hours after the last cycle of stress, mice were asphyxiated, perfused with ice-cold PBS, and brains was collected. Brain samples were homogenized using Glass Potter Elvehjem Tissue Grinder (OMNI International, Kennesaw, GA) and centrifuged at 900g for 6 minutes. Then, cells were pelleted and suspended in 70% isotonic Percoll (GE-Healthcare, Marlborough, MA). This suspension was layered with 50%, 35% and 0% isotonic Percoll to create a discontinuous Percoll gradient. This gradient was centrifuged at 2070g for 20 minutes, and cells were collected from the 70-50% Percoll interface. This interface is enriched with >90% $CD11b^+$ cells (Wohleb et al. 2013).

Isolation of bone marrow and blood cells: Fourteen hours after the last cycle of stress, mice were asphyxiated, and blood and bone marrow samples were collected. Bone marrow was collected from the femur and flushed out with ice-cold PBS. Samples were homogenized using a syringe plunger and filtered through a 70-uM nylon strainer. Blood samples were collected by cardiac puncture into EDTA-lined syringes and red blood cells were lysed using lysis buffer (0.16M NH4Cl, 10mM KHCO3, 0.13mM EDTA). Samples were washed and cells were counted using a BD Coulter Particle Count and Size Analyzer (Beckman Coulter Inc., Pasadena, CA).

Corticosterone ELISA: Blood samples were collected by submandibular bleeding immediately after the last cycle of stress (approximately 7 PM). Plasma was extracted and stored at -80 °C. Corticosterone concentrations were evaluated using the Corticosterone EIA kit (Enzo Inc., Farmingdale, NY; Catalog# ADI-900-097) following manufacturer's instructions.

Real time qPCR from brain and bone marrow samples: Fourteen hours after the last cycle of stress, mice were asphyxiated, and brain and bone marrow samples were collected. For brain mRNA analysis, a 1 mm coronal section of the brain (approximately -0.34 mm to -1.34 mm Bregma) was collected and flash frozen in liquid nitrogen. This brain section, collected using a mouse brain matrix (Kent Scientific, Torrington, CT; Catalog# RBMS-200C), was used to evaluate the general inflammatory profile of the brain following stress and interventions. The rest of the brain was used for isolation of $CD11b^+$ cells for cell flow cytometric analyses. RNA was extracted using a tri-reagent/isopropranolol precipitation protocol (McKim et al. 2016). RNA concentration and quality was determined using the NanoPhotometer (Implen, Munich, Germany). RNA was reverse transcribed into cDNA using a High-Capacity cDNA Reverse

Transcription Kit (Applied Biosystems, Foster City, CA). Real time quantitative PCR was performed using the Applied Biosystems Taqman Gene Expression Assay-on-Demand Gene Expression protocol. Target cDNA and reference cDNA [glyceraldehyde-3-phosphate dehydrogenase (GAPDH)] were amplified simultaneously using a primer/probe set consisting of an oligonucleotide probe with a 5' fluorescent reporter dye (FAM) and a 3' quencher dye (non-fluorescent) for each gene of interest (Life Technologies, Carlsbad, CA). Fluorescence was determined on an ABI PRISM 7300-sequence detection system (Applied Biosystems, Foster City, CA). Data were analyzed using the comparative threshold cycle method, and results were expressed as fold change compared to the reference gene, GAPDH.

For bone marrow mRNA analysis, femurs were flushed with ice-cold PBS and homogenized using a syringe plunger and filtered through a 70 uM strainer. Cells were centrifuged and pelleted into RNA lysis buffer (PrepEase Kit, USB, CA), and RNA isolation was performed according to manufacturer's instructions. RNA concentration and quality was determined using the NanoPhotometry (Implen, Munich, Germany). Reverse transcription and subsequent real time quantitative PCR were performed via the same procedure as for the brain (described above). Because the commonly used housekeeping gene [glyceraldehyde-3-phosphate dehydrogenase (GAPDH)] was altered in the bone marrow by repeated social defeat stress, Eef2 (Eukaryotic translation elongation factor 2) expression was validated and used as reference cDNA for real time quantitative PCR of bone marrow samples. Data were analyzed using the comparative threshold cycle method, and results were expressed as fold change compared to the reference gene, Eef2.

Immunohistochemistry and Digital Image Analysis of ICAM-1 and ΔFosB: Fourteen hours after the last cycle of stress, mice were asphyxiated, transcardially perfused with ice-cold PBS followed by 4% paraformaldehyde. Brain samples were post-fixed in formaldehyde for 24 h, followed by additional 48 h incubation in 30% sucrose at 4°C. Fixed brain samples were frozen with isopentane (-78°C) and dry ice, and stored at -80°C until sectioning. Frozen brain samples were sectioned at 25 μM using a Microm HM550 cryostat (Thermofisher, Dublin, OH) and free-floating sections were preserved in cryoprotectant at -20°C until labeling. Sections were washed in 1X PBS and blocked with 5% normal donkey serum (1%BSA & 0.1% Triton-X in PBS) for an hour at room temperature, followed by an overnight 4°C incubation with primary antibodies: goat anti-ICAM1 (1:500; R&D Systems, Minneapolis, MN; Catalog# AF796, RRID:AB_2248703), rabbit anti-ΔFosB (1:2000; Abcam, Boston, MA; Catalog# ab184938, RRID: AB_2721123) or rabbit anti-Iba1 (1:1000; Wako, Richmond, VA; Catalog# 019-19741, RRID:AB_839504) or rat anti-Ly6C (1:500; Abcam, Boston, MA; Catalog# ab15627, RRID: AB_302004). Sections were washed in 1X PBS and incubated with the corresponding secondary antibodies conjugated with fluorochromes (Alexa Fluor 488 or Alexa Fluor 594). Following 2 hours of incubation at room temperature, sections were washed in DAPI (1:100), then mounted and coverslipped with Fluoromount G (Beckman Coulter Inc., Pasadena, CA), and stored at -20°C. Images were taken on a Zeiss 510 Meta confocal microscope and analyzed using ImageJ software. For the digital imaging analysis of ICAM-1 and Iba1 images, a threshold for positive labeling (full view of the labeled blood vessel, or a full view of labeled microglia with background excluded) was determined for each image. Data were processed by ImageJ using the densitometric scanning of the threshold targets, and results expressed as the average percent area

with positive labeling. For ΔFosB analysis, the number of cells positive for ΔFosB labeling was counted for each image.

Bone marrow processing and immunofluorescent labeling: Immediately after the last cycle of stress, CXCL12-DsRed mice were asphyxiated, transcardially perfused with ice-cold PBS followed by 4% formaldehyde. Femurs were isolated and post-fixed in 4% formaldehyde for 48 h at 4°C. Samples were then transferred into decalcification buffer (0.5 M EDTA in PBS) and incubated at 4°C for 48 hours. Samples were then frozen with isopentane (-78°C) and dry ice and stored at -80°C until sectioning. Next, frozen bone marrow samples were sectioned at 14 μM, collected on Superfrost™ Plus slides (Fisher Scientific, VA), and stored at -20°C. Slides were washed with 1X PBS, incubated with 5% normal donkey serum (1%BSA & 0.1% Triton-X in PBS) for an hour at room temperature, followed by primary antibody rabbit anti-RFP (1:500; Abcam, Boston, MA; Catalog# ab124754, RRID:AB_10971665) incubation overnight at 4°C. Slides were washed in 1X PBS and incubated with an Alexa 594 fluorochrome-conjugated antibody for 2 h at room temperature. Slides were washed, allowed to dry and coverslipped with Fluoromount G (Beckman Coulter Inc., Pasadena, CA), and stored at -20°C. Images were taken using a Zeiss 510 Meta confocal microscope and analyzed using ImageJ software, as described above.

Glucocorticoid (GC) Resistance Assay: Fourteen hours after the last cycle of stress, spleens were collected in ice-cold PBS. Spleen samples were homogenized using a syringe plunger and filtered through a 70 μM strainer. Cells were centrifuged and pelleted into ice-cold Hanks' Balanced Salt Solution (HBSS) to obtain single cell suspensions. Red blood cells were lysed

using the lysis buffer (0.16 M NH4Cl, 10 mM KHCO3, 0.13 mM EDTA), and samples were washed in 10% fetal bovine serum/HBSS. Samples were resuspended in media RPMI 1640 Medium, GlutaMAX^{TM} (ThermoFisher Scientific, Dublin, OH; Catalog# 61870-036) supplemented with 10% fetal bovine serum, 100 U/mL penicillin and 100 µg/mL streptomycin sulfate. Cells (2 X 10^5 per well) were plated in triplicates on a 96 well plate (Corning, Corning, NY; Catalog# 3596). LPS (Sigma, St. Louis, MO; L-2630) was added at 1 µg/mL per well. Corticosterone (Sigma, St. Louis, MO; Catalog# 27840) solutions with 0.2% ethanol were prepared in media and added to the wells at varying concentrations (0, 0.05, 0.1, 0.5 & 5 µM). Cells were cultured with LPS and Corticosterone at 37°C in 5% CO_2 for 18 hours for IL-6 ELISA and for 48 hours for cell viability analysis.

IL-6 ELISA: To determine IL-6 production from splenocytes, supernatant samples were collected 18 hours after culture and incubation (as described above), and stored at -80 °C. IL-6 levels were determined using the BD OptEIA Mouse IL-6 ELISA (BD Biosciences, San Jose, CA) as previously described (Stark et al. 2001). In brief, a 96-well plate was coated with anti-mouse IL-6 capture antibodies and allowed to incubate overnight at 4 °C. Standards (0-1000 pg/mL) and samples were added and incubated for 2 hours at room temperature. Plates were washed and incubated with biotinylated anti-mouse IL-6 antibody. Plates were then incubated with streptavidin-horseradish peroxidase conjugate for 1 hour. Tetramethylbenzidine substrate was added next and reaction was stopped after a 15-minute incubation. Plates were read at 450 nm using a Spectramax plate reader (Molecular Devices, St. Louis, MO). For plasma IL-6 ELISA, Blood samples were collected via cardiac puncture 14 hours after the last cycle of stress, and plasma was stored at -80 °C. IL-6 levels were determined as described above.

Cell viability Assay: Cell viability was assessed as previously described (Hanke et al. 2012). In brief, the Cell Titer 96 aqueous nonradioactive proliferation assay (Promega; Madison, WI) was used to determine cell viability of LPS-activated splenocytes cultured *ex vivo* with corticosterone. At 45 hours following treatment with corticosterone, tetrazolium substrate solution (20 µl) was added to each well. Samples were incubated at 37 °C in 5% CO2 for 3 h, and color changes were quantified by obtaining optical density (OD) readings at 450 nm on the Spectramax plate reader (Molecular Devices, St. Louis, MO). To account for differences in background activity of cells, the mean OD of three control wells were subtracted for a given treatment from each of the corresponding LPS-stimulated values. Control wells contained untreated cells. Results were shown as the percentage of proliferation at baseline (LPS stimulation, no corticosterone treatment).

Statistical Analyses: To test for normal distribution, data were subjected to Shapiro–Wilk test using Statistical Analysis Systems (SAS) statistical software. Observations 2 standard deviations above and below the mean were considered outliers and excluded from subsequent analysis. In total, 22 out of 749 observations were excluded after outlier analysis. To determine significant main effects and interactions between main factors, data were analyzed using two-way (stress × intervention) ANOVA using the General Linear Model procedures of SAS. When there was a main effect of experimental treatment or a treatment interaction effect, differences between group means were evaluated by an F-protected *t* test using the Least-Significant Difference procedure of SAS. *Post hoc* analysis results are depicted graphically in figures. All data are expressed as mean ± SEM.

359 **Results**

360

361 **Stress-induced release of inflammatory monocytes from the bone marrow into circulation**
362 **was prevented by adrenalectomy**. RSD promotes the release of bone marrow-derived
363 monocytes into circulation that are recruited to the brain, augment neuroinflammation, and cause
364 prolonged anxiety-like behavior (Wohleb et al. 2013, McKim et al. 2017). Physiological stress
365 activates the sympathetic nervous system and the HPA axis, both of which play a role in the
366 physiological, immunological, and behavioral responses to stress (Wohleb et al. 2011, Ramirez
367 et al. 2016). Therefore, the aim of this study was to delineate the role of HPA activation and
368 corticosterone production in the physiological and immunological responses to RSD.

369 In the first set of experiments, adrenalectomized (ADX) mice were exposed to stress (six
370 cycles of repeated social defeat), and several physiological and immunological parameters were
371 determined 14 h later. Stress increased plasma corticosterone levels in the sham mice (Fig.1A,
372 $F(1,30)=17.39$; $p < 0.0003$). As expected, removal of the adrenal glands (ADX) ablated this
373 increase (Fig.1A, stress x intervention interaction ($F(1,30)=11.91$; $p < 0.003$). In addition, stress
374 increased plasma IL-6 levels (Fig.1B, $F(1,21)=8.07$; $p < 0.02$) that were prevented in ADX-stress
375 mice compared to sham-stress mice ($p < 0.05$). Stress also increased spleen weight (Fig.1C,
376 $F(1,37)=25.29$; $p < 0.0001$), but this increase was independent of ADX.

377 Stress promotes a profound increase in monocyte and granulocyte production within the
378 bone marrow (Ramirez et al. 2016, McKim et al. 2017). Here, we examined the production of
379 monocytes and granulocytes in adrenalectomized mice after stress exposure. Consistent with
380 previous work (Wohleb et al. 2013), stress increased the percentage of monocytes
381 ($CD11b^{+}/Ly6C^{hi}$) and granulocytes ($CD11b^{+}/Ly6C^{int}$) in the bone marrow (Fig.1D-F, $p < 0.001$,
382 for each). These increases were unaffected by ADX (Fig.1E&F). Stress also increased the

383 percentage of circulating Ly6C^{hi} monocytes (Fig.1G&H, $F(1,22)=16.99$; $p < 0.006$). Post hoc
384 analysis revealed that ADX-stress mice had significantly fewer circulating monocytes than
385 sham-stress mice ($p < 0.005$). Overall, ADX attenuated corticosterone production during stress
386 and reduced the release of inflammatory monocytes into circulation without altering their
387 production in the bone marrow.
388
389 **Stress-associated reduction of CXCL12 in the bone marrow was attenuated by**
390 **adrenalectomy.** We show that ADX prevented the release of monocytes into circulation, but did
391 not alter their production in the bone marrow (Fig.1). Therefore, we sought to determine if the
392 reduced release of monocytes in ADX mice was associated with altered CXCL12 expression, a
393 key chemokine important for the retention of hematopoietic stem cells and monocytes in the
394 bone marrow (Heidt et al. 2014). First, CXCL12-DsRed mice were exposed to stress, and
395 CXCL12 protein levels were determined in the bone marrow. Fig.2A shows that stress caused a
396 marked reduction in CXCL12 protein expression in the bone marrow. This effect was paralleled
397 in wild-type mice that had a significant reduction in CXCL12 mRNA in the bone marrow after
398 RSD (Fig.2B, $p < 0.005$). In a separate experiment, mice were adrenalectomized (ADX) prior to
399 exposure to stress and CXCL12 mRNA expression was determined in the bone marrow. Again,
400 stress reduced CXCL12 mRNA expression in the bone marrow (Fig.2C, $F(1,16)=5.36$, $p < 0.05$).
401 In addition, ADX increased bone marrow CXCL12 mRNA (Fig. 2C, $F(1,16)=10.70$; $p < 0.01$).
402 *Post hoc* analysis confirmed that sham-stress mice had lower CXCL12 mRNA expression
403 compared to sham-control mice ($p < 0.05$), and this reduction was not evident in ADX-stress
404 mice compared to ADX-control. Taken together, stress reduced CXCL12 expression in the bone
405 marrow and this reduction was prevented by ADX.

406 **Stress-induced monocyte accumulation in the brain and the neurovascular induction of**
407 **intercellular adhesion molecule-1 (ICAM-1) was prevented by adrenalectomy.** Next, we
408 assessed the effects of adrenalectomy (ADX) and stress on monocyte accumulation in the brain
409 and endothelial ICAM-1 induction. Corresponding with our previous reports (McKim et al.
410 2016, McKim et al. 2017), stress increased the presence of monocytes ($CD11b^{+}/CD45^{hi}$) in the
411 brain (Fig.3A&B, $F(1,23)=34.28$, $p < 0.0002$). This monocyte accumulation in the brain with
412 stress tended to be attenuated by ADX (Fig.3A&B, stress x intervention ($F(1,23)=4.07$; $p =$
413 0.06). *Post hoc* analysis confirmed that ADX-stress mice had significantly fewer monocytes in
414 the brain compared to sham-stress mice ($p < 0.02$).

415 We next determined mRNA expression of several key inflammatory mediators, IL-1β,
416 TLR4, and ICAM-1, in a coronal brain section collected from the same mice used in the flow
417 cytometric analysis above. The coronal section was used to evaluate the general inflammatory
418 profile of the brain following stress and interventions. While ADX reduced TLR4 mRNA levels
419 in the brain (Fig.3C, $F(1,12)=74.89$; $p < 0.0001$), there was no main effect of stress on TLR4
420 mRNA expression. Stress also increased IL-1β mRNA expression in the brain (Fig.3D,
421 $F(1,35)=20.47$; $p < 0.0001$), but this increase was independent of ADX (Fig.3D). Stress
422 increased ICAM-1 levels in the brain (Fig.3E, $F(1,14)=10.51$; $p < 0.01$), and this induction was
423 attenuated by ADX. *Post hoc* analysis revealed that ADX-stress mice tended to have lower
424 mRNA expression of ICAM-1 compared to sham-stress mice ($p = 0.06$).

425 Last, intercellular adhesion molecule-1 (ICAM-1) protein expression was determined
426 with ADX and stress. The recruitment/accumulation of monocytes was associated with increased
427 ICAM-1 expression in the brain endothelial cells. The selective expression of ICAM-1 labeling
428 on endothelial cells was confirmed by co-labeling with Ly6C. Ly6C is strongly expressed on

endothelial cells and remains unaltered during inflammatory events (Jutila et al. 1988, Wohleb et al. 2013, Zhang et al. 2014, Liu et al. 2015). In the current study, Ly6C expression on the brain endothelial cells was unaffected by stress or adrenalectomy (data not shown). Here, ICAM-1 expression was increased with stress in the dentate gyrus (Fig.3F&G, $F(1,11)=7.29$; $p < 0.05$) and prelimbic cortex (Fig.3H, $F(1,15)=8.26$; $p < 0.05$). *Post hoc* analysis confirmed that ICAM-1 expression was significantly higher in the sham-stress mice compared to ADX-stress in the dentate gyrus ($p < 0.02$) and tended to be higher in the prelimbic cortex ($p=0.06$). Collectively, increased monocyte recruitment/accumulation and ICAM-1 induction in the brain endothelial cells during stress were attenuated by adrenalectomy.

Stress-induced release of inflammatory monocytes from the bone marrow into circulation was attenuated by metyrapone. We show that adrenalectomy prevented the stress-induced release of inflammatory monocytes into circulation. ADX, however, may exert broad effects on homeostatic endocrine functioning (Cruz-Topete et al. 2016). Therefore, metyrapone (MTP) intervention was used during stress to ablate corticosterone production. Metyrapone prevents corticosterone synthesis by inhibiting 11β-hydroxylase, the enzyme that converts inert corticosterone into active corticosterone (Garcia-Garcia et al. 2017). Here, mice were treated with vehicle or MTP 30 min prior to each cycle of social defeat, and several physiological and immune parameters were determined 14 h after stress. First, stress-induced neuronal activation (i.e., ΔFosB expression) within threat appraisal centers was determined with or without MTP intervention. Notably, ΔFosB (an isoform of FosB) is an immediate early gene detected in neurons (Perrotti et al. 2004), and has a longer half-life compared to other immediate early genes (e.g. c-Fos) (McClung et al. 2004). Therefore, it serves as a marker of cumulative neuronal

activation over the six days of repeated social defeat stress (McKim et al. 2017). Here, we show that stress increased neuronal activation (i.e., ΔFosB expression) in the prelimbic cortex (Fig.4A&B, ($F(1,11)=17.69$, $p < 0.01$) and this increase was maintained independent of MTP intervention.

Next, plasma corticosterone and spleen weight were assessed after stress and MTP intervention. Similar to the ADX experiment, stress increased plasma corticosterone levels (Fig.4C, $F(1,22)=22.21$; $p < 0.0002$) and this increase was attenuated by MTP (Fig.4C, stress x intervention ($F(1,22)=13.31$, $p < 0.002$). Parallel to this, stress increased plasma IL-6 (Fig.4D, $F(1,14)=7.38$; $p < 0.05$), which was also attenuated by MTP. For example, *post hoc* analysis revealed that MTP-stress mice had significantly lower IL-6 levels in the plasma compared to vehicle-stress mice ($p < 0.05$). Stress also increased spleen weight (Fig.4E, ($F(1,26)=48.31$; $p < 0.0001$), but this increase was independent of MTP. Taken together, MTP attenuated activation of the HPA axis during stress, without affecting threat appraisal (neuronal activation) of the stressor.

Next, we assessed the effects of MTP intervention on monocyte production and release in response to stress. Consistent with the ADX results, stress increased the production of monocytes ($CD11b^{+}/Ly6C^{hi}$) and granulocytes ($CD11b^{+}/Ly6C^{int}$) in the bone marrow (Fig.4F&G, $p < 0.001$, for each), but these increases were unaffected by MTP intervention. Nonetheless, the stress-induced release of $Ly6C^{hi}$ monocytes in circulation (Fig.4H&I, $F(1,23)=86.41$; $p < 0.0001$) was attenuated by MTP intervention (Fig.4H&I, stress x intervention, $F(1,23)=5.30$; $p < 0.05$). More specifically, the percentage of circulating $Ly6C^{hi}$ monocytes was lower in the MTP-treated stress mice compared to the vehicle-treated stress mice ($p < 0.0005$), but these levels were still higher than in control mice ($p < 0.0001$). Last, we determined the effects of stress and MTP

intervention on CXCL12 expression, a key retention factor for bone marrow stem cells and monocytes. Stress reduced CXCL12 mRNA levels in the bone marrow (Fig.4J, ($F(1,9)=11.99$; $p < 0.05$) in an MTP-dependent manner (Fig.4J, stress x intervention, ($F(1,9)=5.62$; $p < 0.05$). *Post hoc* analysis confirmed that CXCL12 mRNA levels in the bone marrow were significantly reduced in the vehicle-stress mice compared to vehicle-controls ($P < 0.05$). Moreover, CXCL12 mRNA levels in the bone marrow of MTP-stress mice were not different compared to MTP-controls (Fig.4J). Overall, MTP intervention during stress reduced the release of inflammatory monocytes into circulation by increasing their retention in the bone marrow.

Metyrapone attenuated stress-induced glucocorticoid resistance of splenocytes. We have previously reported that myeloid cells from the spleen of mice exposed to RSD have an exaggerated inflammatory response to LPS stimulation and a resistance to the suppressive effects of corticosterone (i.e, glucocorticoid resistance) (Stark et al. 2001, Hanke et al. 2012). Here, we examined the effects of MTP on stress-induced glucocorticoid resistance of splenocytes. In this experiment, splenocytes were collected 14 h after stress, cultured *ex vivo*, activated with LPS, and incubated with increasing concentrations of corticosterone. Fig.5A shows that an increasing concentration of corticosterone from 0 μM (baseline) to 5 μM reduced the survival of LPS-activated splenocytes from vehicle-control and MTP-control groups. The LPS-activated splenocytes from vehicle-stress group had a higher rate of survival (i.e. glucocorticoid resistance) under all concentrations of corticosterone when compared to vehicle-controls ($p < 0.01$ for each dose). Moreover, the ability of corticosterone to reduce survival of splenocytes was dependent on MTP intervention (Fig.5A, stress x intervention, $F(1,18)=6.28$; $p < 0.05$). For example, cell survival of the splenocytes from the MTP-stress group was reduced by corticosterone at 0.5 μM

($p < 0.05$) and 5 μM ($p < 0.01$) compared to the vehicle-stress group. These findings indicate that the increased glucocorticoid resistance of splenocytes following exposure to stress was attenuated by MTP intervention.

Next, in order to assess the effect of stress and MTP on the inflammatory capacity of splenocytes, IL-6 levels were determined in supernatants from the duplicate preparation of the same *ex vivo* cultures as described above. LPS-activated splenocytes from vehicle-stress mice produced significantly higher IL-6 in presence of corticosterone compared to vehicle-control mice ($p < 0.0001$, for all concentrations). Furthermore, this IL-6 response was significantly reduced with MTP intervention (Fig. 5B, stress x intervention, $F(1,11)=6.72$; $p < 0.05$). Compared to MTP-stress, LPS-activated splenocytes from vehicle-stress mice produced the highest IL-6 levels in the presence of corticosterone ($p < 0.007$ at 0 μM; $p < 0.02$ at 0.05 μM; $p < 0.0003$ at 0.1 μM; $p < 0.0001$ at 0.5 μM & $p < 0.001$ at 5 μM). Overall, stress augmented the proinflammatory response of splenocytes to LPS, and that these splenocytes were resistant to the anti-inflammatory actions of corticosterone. Furthermore, the stress-induced exaggerated inflammatory response to LPS was attenuated by MTP intervention.

Metyrapone attenuated monocyte recruitment to the brain and prevented neuroinflammatory signaling. Next, the effects of stress and MTP intervention on microglial morphology, monocyte accumulation in the brain, and inflammation were assessed. As expected, stress increased the morphological restructuring of microglia (i.e., increased % area of Iba-1 labeling) in the dentate gyrus (Fig.6A&B, $F(1,11)=9.17$; $p < 0.02$). There was no difference in the morphological restructuring of microglia between MTP-treated control and MTP-treated stress mice ($p = 0.29$). Stress also increased microglial restructuring in the prelimbic cortex

(Fig.6C, $F(1,11)=6.82$; $p < 0.05$), and this increase was prevented by MTP intervention (Fig.6C, stress x intervention, $F(1,11)=6.82$; $p <0.05$). For example, vehicle-treated stress mice showed higher Iba-1 expression of microglia compared to MTP-treated stress mice ($p < 0.05$). Therefore, MTP intervention during stress may lead to region-dependent reductions in the morphological alterations of microglia.

Next, we examined monocyte recruitment to the brain with MTP intervention during stress. MTP attenuated the stress-induced accumulation of monocyte/macrophages ($CD11b^{+}/CD45^{hi}$) in the brain (Fig.6D&E, stress x intervention, $F(1,11)=8.75$; $p < 0.001$). For example, vehicle-stress mice had significantly more monocytes in the brain compared to MTP-stress mice (Fig.6B, $p < 0.005$). MTP-stress mice, however, still had more monocytes in the brain than control mice ($p < 0.05$). In the same experiments, mRNA expression of inflammatory mediators, TLR4, IL-1β and ICAM-1 were also determined in a coronal section of the brain. TLR4 mRNA levels were unaffected by either stress or MTP treatment (Fig.6F). IL-1β mRNA levels were increased in the brain after stress (Fig.6G, $F(1,24)=11.43$; $p < 0.0028$), and this increase was attenuated by MTP (Fig.6G, stress x intervention, $(F(1,24)=4.19$; $p = 0.05)$. For example, vehicle-stress mice had significantly higher IL1β mRNA levels in the brain ($p < 0.01$) compared to MTP-stress mice. ICAM-1 mRNA in the brain was also increased by stress (Fig.6H, $F(1,22)=7.29$; $p < 0.01$) and this increase was prevented by MTP (Fig.6H, stress x intervention, $F(1,22)=20.96$; $p < 0.001$). For instance, vehicle-stress mice had significantly higher ICAM-1 mRNA ($p < 0.0001$) compared to MTP-stress mice. Taken together, MTP prevented stress-induced morphological changes in microglia, recruitment of monocytes, ICAM-1 and IL1β mRNA induction in the brain.

Metyrapone prevented stress-induced induction of endothelial intercellular cell adhesion molecule-1 (ICAM-1) in the brain. Last, the effects of stress and MTP intervention on ICAM-1 induction were assessed. As indicated by ICAM-1 expression on Ly6C+ brain endothelial cells, there was a neurovascular induction of ICAM-1 protein by stress in the dentate gyrus (Fig.7A&B, $F(1,11)=15.41$; $p < 0.006$) and prelimbic cortex (Fig.7C, $F(1,11)=6.21$; $p < 0.05$). Furthermore, this increase was attenuated by MTP intervention (Fig.7A&B, stress x intervention, $F(1,11)=24.81$, $p < 0.002$ for DG & Fig.7C, ($F(1,11)=7.09$, $p < 0.03$ for PrL). Vehicle-stress mice had a higher ICAM-1 protein expression compared to MTP-stress mice in the dentate gyrus ($p < 0.01$) and in the prelimbic cortex ($p < 0.05$). Thus, MTP intervention was effective in preventing stress-induced ICAM induction within threat appraisal centers.

Discussion

We and others have reported that repeated social defeat stress enhanced the production and release of inflammatory monocytes that accumulate in the brain (Wohleb et al. 2013, Menard et al. 2017). RSD also induced endothelial cell adhesion molecule expression and microglial activation, marked by the production of chemokines and pro-inflammatory mediators. This microglial activation was associated with the recruitment of monocytes that induced neuroinflammatory signaling and anxiety-like behavior (McKim et al. 2017). Activation of the peripheral immune compartments during RSD occurred through the sympathetic nervous system (SNS) and the HPA axis (Hanke et al. 2012, Ramirez et al. 2016). Our objective here was to delineate the effects of HPA activation and corticosterone on immune dysregulation during RSD. We report that corticosterone produced during stress did not alter monocyte production in the bone marrow, but promoted their release into circulation in a CXCL12-dependent manner. Corticosterone also enhanced neuroendothelial ICAM-1 expression that was associated with

568 increased accumulation of monocytes and enhanced IL-1β production in the brain. Last,
569 corticosterone production during stress was responsible for glucocorticoid resistance in the
570 splenic myeloid cells.

571 An important confirmation from this study was that stress-induced HPA activation
572 resided downstream of the threat appraisal circuitry. RSD increases the number of ΔFosB and
573 cFos-positive cells in the threat appraisal regions, including prelimbic cortex, hippocampus and
574 amygdala (Wohleb et al. 2011, McKim et al. 2017). Noradrenergic and GABAergic interventions
575 (Wohleb et al. 2011, Ramirez et al. 2016) prevented this stress-induced threat appraisal
576 activation, which also prevented monocyte release and accumulation in the brain. Because stress
577 activates both the SNS and HPA axis, our goal was to intervene in the stress-response pathway at
578 the level of corticosterone production, a physiological hallmark of stress response (Sapolsky et
579 al. 2000). Corticosterone depletion prevented the increase in plasma corticosterone and IL-6
580 during stress, but did not alter neuronal activation in the threat appraisal regions. These findings
581 indicate that threat appraisal activation during stress preceded HPA activation and corticosterone
582 production.

583 A key finding of this study was that corticosterone depletion prevented the stress-induced
584 release of bone marrow-derived monocytes into circulation. It is important to note that enhanced
585 production of monocytes with stress was maintained despite corticosterone depletion. These
586 findings to indicate that corticosterone depletion increased monocyte retention within the bone
587 marrow during stress. In support of this conclusion, we show novel data that stress induced a
588 profound reduction in CXCL12 mRNA and protein in the bone marrow. CXCL12 is a
589 chemokine key in the retention of bone marrow cells. Disruption in the CXCL12/CXCR4
590 pathways caused significant impairments in cell mobilization from the bone marrow (Levesque

591 et al. 2003, Greenbaum et al. 2013). CXCL12 levels in the brain were not determined in the
592 current study, but we have previously shown that brain CXCL12 levels remain unaltered by
593 stress (Sawicki et al. 2014). In the current study, adrenalectomy and metyrapone intervention
594 attenuated the stress-induced reduction of CXCL12 in the bone marrow, and this effect was
595 associated with reduced monocyte release into circulation.

596 Our findings on the role of corticosterone in monocyte mobilization are novel because
597 existing literature attributes mobilization of bone marrow cells to macrophages or noradrenergic
598 nerve terminals at the bone marrow (Katayama et al. 2006, Chow et al. 2011). For instance, local
599 sympathetic activity in the bone marrow was associated with increased production and release of
600 hematopoietic stem cells and monocytes during steady state and chronic variable stress (Mendez-
601 Ferrer et al. 2010, Heidt et al. 2014). Nonetheless, the mechanisms underlying mobilization of
602 monocytes during psychological stress are unclear. For instance, acute psychological stress, but
603 not adrenergic receptor activation, increased progenitor cell release into circulation (Riddell et al.
604 2015). Moreover, transgenic mice with deficits in hematopoietic stem cell mobilization recover
605 normal functions when parabiotically paired with wildtype mice (Pierce et al. 2017). These
606 studies showed that a blood-borne factor, i.e. corticosterone, mobilizes bone marrow stem cells
607 into circulation (Pierce, 2017). Our findings here show that corticosterone plays an important
608 role in mobilization of bone marrow monocytes during stress.

609 Related to the points above, monocyte production during stress has been attributed to
610 enhanced sympathetic signaling in the bone marrow (Heidt et al. 2014). We have reported that
611 interrupting the sympathetic pathway prevents production of monocytes and accumulation in
612 tissues (Wohleb et al. 2011, Powell et al. 2013). In the current study, corticosterone depletion did
613 not completely ablate monocyte release. Thus, the SNS likely remains at play. We propose that

614 corticosterone does not contribute to enhanced monocyte production during stress, but acts
615 synergistically with the SNS to promote monocyte release into circulation.

616 Another noteworthy finding of this study was that corticosterone depletion attenuated
617 ICAM-1 expression on the neurovascular endothelial cells in response to stress. We and others
618 have previously reported that stress causes rapid induction of ICAM-1 on the vascular
619 endothelium (Joachim et al. 2008, Sawicki et al. 2014). Blocking threat appraisal activation
620 during stress prevented ICAM-1 induction (McKim et al. 2017). Nonetheless, preventing
621 microglial activation or eliminating microglia did not alter the stress-induced increase in ICAM-
622 1 (McKim et al. 2017). Therefore, we hypothesized that corticosterone, which is produced
623 rapidly during stress, promotes ICAM-1 induction in the neurovascular endothelium. In support
624 of this hypothesis, both adrenalectomy and metyrapone intervention prevented the stress-induced
625 increase in ICAM-1. Corresponding with reduced ICAM-1 expression, the percentage of $CD45^{hi}$
626 monocytes in the brain was also reduced with corticosterone depletion. Collectively,
627 corticosterone depletion during stress prevents monocyte accumulation in the brain by limiting
628 their release into circulation and by reducing their adherence to ICAM-1 on the brain endothelial
629 cells.

630 It is also relevant to discuss that reduced monocyte accumulation in the brain with
631 metyrapone was associated with reduced IL-1β mRNA expression. This is consistent with our
632 previous studies showing that monocytes accumulate in the brain during stress and propagate IL-
633 1 signaling through the endothelial IL1-receptor1 on the brain vasculature (McKim et al. 2017).
634 In addition, monocyte accumulation and increased IL-1β expression may further augment
635 microglial activation with stress. This was apparent in the prelimbic cortex where metyrapone
636 attenuated monocyte accumulation in the brain and prevented morphological alterations of

637 microglia. In the adrenalectomized mice, microglial activation was not assessed and stress-
638 induced IL-1β mRNA was maintained despite reduction of monocyte accumulation. This
639 discrepancy in IL-1β expression between adrenalectomy and metyrapone treatment may be
640 attributed to broader effects of adrenalectomy (Cruz-Topete et al. 2016). For instance,
641 adrenalectomized, but not metyrapone-treated, mice had reduced CX3CR1, nr4a1 and P2X7
642 mRNA expression in the brain at baseline (data not shown). Thus, adrenalectomy may introduce
643 confounds that influence CNS homeostasis. Nonetheless, our overall results support the
644 conclusion that corticosterone induction with RSD is critical in the release of pro-inflammatory
645 and glucocorticoid resistant monocytes that subsequently accumulate in the brain and augment
646 neuroinflammatory signaling.

647 It is also important to note that metyrapone blocks corticosterone production by
648 preventing the conversion of its precursor, 11β-deoxycorticosterone, levels of which are
649 increased following metyrapone treatment. Although 11β-deoxycorticosterone may exert
650 aldosterone-like effects, its potency is low (2% potency as aldosterone) and is not expected to
651 cause significant effects (Gomez-Sanchez et al. 2014). Furthermore, 11β-deoxycorticosterone
652 levels would not be increased with adrenalectomy. Indeed, our findings from the adrenalectomy
653 and metyrapone experiments are consistent with each other. Thus, the results of this study were
654 not confounded by increased 11β-deoxycorticosterone levels with metyrapone treatment.

655 Another important finding here was that corticosterone depletion prevented stress-
656 induced glucocorticoid resistance in the splenocytes. Glucocorticoids suppress inflammatory
657 signaling by preventing transcription and posttranslational modification of inflammatory genes
658 and by triggering apoptosis of immune cells. (Smoak et al. 2004). Chronic stress in humans
659 blunts the ability of glucocorticoids to suppress inflammatory signaling, and increases risk for

viral infections, cardiovascular and other chronic inflammatory conditions (Cohen et al. 2012, Fagundes et al. 2013, Heidt et al. 2014, Miller et al. 2014). Glucocorticoid resistance in RSD was shown in splenocytes that were resistant to the apoptotic effects of corticosterone and produced exaggerated levels of IL-6 in response to LPS (Stark et al. 2001, Quan et al. 2003). This glucocorticoid resistance is caused by a failure of the glucocorticoid receptor in myeloid cells to translocate into the nucleus (Quan et al. 2003). Nonetheless, the role of corticosterone on glucocorticoid resistance in these myeloid cells was unknown. Here, we provide novel data that glucocorticoid resistance of myeloid cells was caused by overproduction of corticosterone during stress. Indeed, stress-induced glucocorticoid resistance of myeloid cells was prevented by corticosterone depletion with metyrapone. Thus, HPA activation and corticosterone production during stress induces glucocorticoid resistance in myeloid cells.

In conclusion, we shed light on the specific role of corticosterone in the immunomodulatory effects of RSD. We show for the first time that corticosterone production during stress contributes to monocyte mobilization from the bone marrow by reducing CXCL12. Furthermore, corticosterone also increases neurovascular ICAM-1 expression during stress that facilitates monocyte adherence to vasculature. Finally, our findings indicate that corticosterone production during RSD is the cause of glucocorticoid resistance in myeloid cells. These findings have implications not only in stress-induced neuropsychiatric conditions, but also in cardiovascular and inflammatory disorders associated with stress.

680 **Figure Legends:**

681

682 **Figure 1. Stress-induced release of inflammatory monocytes from the bone marrow into**
683 **circulation was prevented by adrenalectomy**. Male C57BL/6 mice were subjected to sham or
684 adrenalectomy (ADX) surgery and allowed to recover until exposure to repeated social defeat
685 (Stress). Plasma for corticosterone was collected immediately after stress, and plasma for IL-6,
686 bone marrow and blood samples were collected 14 h later. A) Corticosterone levels (n=9) and
687 B) IL-6 levels (n=6) in the plasma, and C) spleen weight (n=9) were determined. D)
688 Representative bivariate dot plots of monocytes ($CD11b^{+}$ $Ly6C^{hi}$) and granulocytes ($CD11b^{+}$
689 $Ly6C^{int}$) in the bone marrow are depicted. Percentage of bone marrow E) monocytes and F)
690 granulocytes (n=6). G) Representative bivariate dot plots of CD11b and Ly6C labeling of
691 monocytes in circulation. H) Percentage of $Ly6C^{hi}$ monocytes in the blood (n=6). Bars represent
692 mean ± SEM. Means with different letters (a, b, or c) are significantly different ($p < 0.05$) from
693 each other.

694

695 **Figure 2. Stress-associated reduction of CXCL12 in the bone marrow was attenuated by**
696 **adrenalectomy.** Male CXCL12-DsRed mice were exposed to control or repeated social defeat
697 (Stress). A) Representative images of RFP expression in the femur immediately after stress
698 (n=3), scale bar = 125 μm. Next, male C57BL/6 mice were exposed to control or repeated social
699 defeat (Stress) and B) CXCL12 mRNA expression in the bone marrow was determined (n=3). In
700 a separate experiment, male C57BL/6 mice were subjected to sham or adrenalectomy (ADX)
701 surgery and allowed to recover until exposure to repeated social defeat (Stress) C) CXCL12

mRNA expression in the bone marrow 14 h later (n=6). Bars represent mean ± SEM. Means with different letters (a, b, or c) are significantly different ($p < 0.05$) from each other.

Figure 3. Stress-induced monocyte accumulation in the brain and the neurovascular induction of intercellular adhesion molecule-1 (ICAM-1) was prevented by adrenalectomy. Male C57BL/6 mice were subjected to sham or adrenalectomy (ADX) surgery and allowed to recover until exposure to repeated social defeat (Stress). Brain samples were collected 14 h later for flow cytometry and mRNA analyses. A) Representative bivariate dot plots and B) percentage of CD45 and CD11b labeling of Percoll-enriched myeloid cells isolated from the brain are depicted (n=6). mRNA expression of C) TLR4, D) IL-1β and E) ICAM-1 in a coronal brain section (n=3-6). In a separate experiment, mice were treated as above. At 14 h after stress, brains were perfused, fixed and labeled for ICAM-1 expression (n=6). F) Representative images of ICAM-1 and Ly6C expression on blood vessels counterstained with DAPI in the dentate gyrus, scale bar = 275 µm. Inset indicates region used for analysis. Percent area of ICAM-1 labeling in the G) dentate gyrus and H) prelimbic cortex (PrL) are depicted. Bars represent mean ± SEM. Means with different letters (a, b, or c) are significantly different ($p < 0.05$) from each other. Inset indicates region from which images were acquired.

Figure 4. Stress-induced release of inflammatory monocytes from the bone marrow into circulation was attenuated by metyrapone. Male C57BL/6 mice were injected daily with either vehicle or metyrapone (100mg/kg) 30 minutes prior to control or repeated social defeat (Stress). At 14 h after stress, brains were perfused, fixed, and labeled for ΔFosB. A) Representative images of ΔFosB expression in the prelimic cortex (PrL), scale bar = 125 µm.

Inset indicates region used for analysis. B) Average number of $\Delta FosB^+$ cells in the prelimbic cortex is shown (n=3). C) Plasma corticosterone (n=6) and D) IL-6 levels (n=3-4) are shown. E) Spleen weight (n=6) was determined. Percentage of F) $CD11b^+$ $Ly6C^{hi}$ monocytes and G) $CD11b^+$ $Ly6C^{int}$ granulocytes in the bone marrow. H) Percentage and I) Representative bivariate dot plots of $CD11b^+$ and $Ly6C^{hi}$ labeling of monocytes in circulation. J) mRNA expression of CXCL12 in the bone marrow (n=3-4). Bars represent mean ± SEM. Means with different letters (a, b, or c) are significantly different ($p < 0.05$) from each other.

Figure 5. Metyrapone attenuated stress-induced glucocorticoid resistance of splenocytes. Male C57BL/6 mice were injected daily with either vehicle or metyrapone (100 mg/kg) 30 minutes prior to control or repeated social defeat (Stress). Splenocytes were collected 14 h later, and cultured *ex vivo* in presence of LPS (1µg/mL) and increasing concentrations of corticosterone (0, 0.05, 0.1, 0.5 & 5 µM). A) Cell survival was determined 48 h after treatment and results are expressed as percent baseline of cell survival at 0 µM corticosterone (as indicated by the horizontal dashed line) (n=6) B) Supernatant samples were collected from a duplicate preparation 18 hour after the beginning of culture, and IL-6 levels were determined (n=3). Bars represent mean ± SEM. Means with different letters (a, b, or c) are significantly different ($p < 0.05$) from each other.

Figure 6. Metyrapone attenuated monocyte recruitment to the brain and prevented neuroinflammatory signaling. Male C57BL/6 mice were injected daily with either vehicle or metyrapone (100 mg/kg) 30 minutes prior to control or repeated social defeat (Stress). At 14 h after stress, brains were perfused, fixed, and labeled for Iba-1. A) Representative images of Iba-1

expression in the dentate gyrus (10X), Scale bar = 275 μm. Inset indicates region used for analysis. Percent area of Iba-1 labeling in the B) dentate gyrus and C) prelimbic cortex (PrL) (n=3-4). In a separate experiment, mice were treated as above. D) Representative bivariate dot plots of CD45 and CD11b labeling of Percoll-enriched myeloid cells isolated from the brain. E) The percentage of $CD45^{hi}$ monocytes/macrophages in the enriched $CD11b^{+}$ from the brain (n=3). mRNA expression of F) TLR4, G) IL-1β and H) ICAM-1 in a coronal brain section (n=3-6). Bars represent mean ± SEM. Means with different letters (a, b, or c) are significantly different ($p < 0.05$) from each other.

Figure 7. Metyrapone prevented stress-induced induction of endothelial intercellular cell adhesion molecule-1 (ICAM-1) in the brain. Male C57BL/6 mice were injected daily with either vehicle or metyrapone (100 mg/kg) 30 minutes prior to control or repeated social defeat (Stress). At 14 h after stress, brains were perfused, fixed, and labeled for ICAM-1 expression. A) Representative images of ICAM-1 and Ly6C expression on blood vessels counterstained with DAPI in the dentate gyrus, Scale bar = 275 μm. Inset indicates region used for analysis. Percent area of ICAM-1 labeling in the B) dentate gyrus and C) prelimbic cortex (PrL) (n=3-4). Bars represent mean ± SEM. Means with different letters (a, b, or c) are significantly different ($p < 0.05$) from each other.

References

Avitsur, R., J. L. Stark and J. F. Sheridan (2001). "Social stress induces glucocorticoid resistance in subordinate animals." Horm Behav **39**(4): 247-257.

Chow, A., D. Lucas, A. Hidalgo, S. Mendez-Ferrer, D. Hashimoto, C. Scheiermann, M. Battista, M. Leboeuf, C. Prophete, N. van Rooijen, M. Tanaka, M. Merad and P. S. Frenette (2011). "Bone marrow CD169+ macrophages promote the retention of hematopoietic stem and progenitor cells in the mesenchymal stem cell niche." J Exp Med **208**(2): 261-271.

Cohen, S., D. Janicki-Deverts, W. J. Doyle, G. E. Miller, E. Frank, B. S. Rabin and R. B. Turner (2012). "Chronic stress, glucocorticoid receptor resistance, inflammation, and disease risk." Proc Natl Acad Sci U S A **109**(16): 5995-5999.

Cruz-Topete, D., P. H. Myers, J. F. Foley, M. S. Willis and J. A. Cidlowski (2016). "Corticosteroids Are Essential for Maintaining Cardiovascular Function in Male Mice." Endocrinology **157**(7): 2759-2771.

Dhabhar, F. S., W. B. Malarkey, E. Neri and B. S. McEwen (2012). "Stress-induced redistribution of immune cells--from barracks to boulevards to battlefields: a tale of three hormones--Curt Richter Award winner." Psychoneuroendocrinology **37**(9): 1345-1368.

Fagundes, C. P., R. Glaser and J. K. Kiecolt-Glaser (2013). "Stressful early life experiences and immune dysregulation across the lifespan." Brain Behav Immun **27**(1): 8-12.

Garcia-Garcia, L., A. A. Shiha, R. Fernandez de la Rosa, M. Delgado, A. Silvan, P. Bascunana, J. P. Bankstahl, F. Gomez and M. A. Pozo (2017). "Metyrapone prevents brain damage induced by status epilepticus in the rat lithium-pilocarpine model." Neuropharmacology **123**: 261-273.

Gomez-Sanchez, E. and C. E. Gomez-Sanchez (2014). "The multifaceted mineralocorticoid receptor." Compr Physiol **4**(3): 965-994.

Greenbaum, A., Y. M. Hsu, R. B. Day, L. G. Schuettpelz, M. J. Christopher, J. N. Borgerding, T. Nagasawa and D. C. Link (2013). "CXCL12 in early mesenchymal progenitors is required for haematopoietic stem-cell maintenance." Nature **495**(7440): 227-230.

Hanke, M. L., N. D. Powell, L. M. Stiner, M. T. Bailey and J. F. Sheridan (2012). "β-adrenergic blockade decreases the immunomodulatory effects of social disruption stress." Brain Behav Immun.

Heidt, T., H. B. Sager, G. Courties, P. Dutta, Y. Iwamoto, A. Zaltsman, C. von Zur Muhlen, C. Bode, G. L. Fricchione, J. Denninger, C. P. Lin, C. Vinegoni, P. Libby, F. K. Swirski, R. Weissleder and M. Nahrendorf (2014). "Chronic variable stress activates hematopoietic stem cells." Nat Med **20**(7): 754-758.

Jacobson, L., S. F. Akana, C. S. Cascio, J. Shinsako and M. F. Dallman (1988). "Circadian variations in plasma corticosterone permit normal termination of adrenocorticotropin responses to stress." Endocrinology **122**(4): 1343-1348.

Joachim, R. A., B. Handjiski, S. M. Blois, E. Hagen, R. Paus and P. C. Arck (2008). "Stress-induced neurogenic inflammation in murine skin skews dendritic cells towards maturation and migration: key role of intercellular adhesion molecule-1/leukocyte function-associated antigen interactions." Am J Pathol **173**(5): 1379-1388.

Jutila, M. A., F. G. Kroese, K. L. Jutila, A. M. Stall, S. Fiering, L. A. Herzenberg, E. L. Berg and E. C. Butcher (1988). "Ly-6C is a monocyte/macrophage and endothelial cell differentiation antigen regulated by interferon-gamma." Eur J Immunol **18**(11): 1819-1826.

Katayama, Y., M. Battista, W. M. Kao, A. Hidalgo, A. J. Peired, S. A. Thomas and P. S. Frenette (2006). "Signals from the sympathetic nervous system regulate hematopoietic stem cell egress from bone marrow." Cell **124**(2): 407-421.

Kendler, K. S., L. M. Karkowski and C. A. Prescott (1999). "Causal relationship between stressful life events and the onset of major depression." Am J Psychiatry **156**(6): 837-841.

817 Lehmann, M. L., R. A. Brachman, K. Martinowich, R. J. Schloesser and M. Herkenham (2013).
818 "Glucocorticoids orchestrate divergent effects on mood through adult neurogenesis." J Neurosci **33**(7):
819 2961-2972.
820 Levesque, J. P., J. Hendy, Y. Takamatsu, P. J. Simmons and L. J. Bendall (2003). "Disruption of the
821 CXCR4/CXCL12 chemotactic interaction during hematopoietic stem cell mobilization induced by GCSF or
822 cyclophosphamide." J Clin Invest **111**(2): 187-196.
823 Liu, X., T. Yamashita, Q. Chen, N. Belevych, D. B. McKim, A. J. Tarr, V. Coppola, N. Nath, D. P. Nemeth, Z.
824 W. Syed, J. F. Sheridan, J. P. Godbout, J. Zuo and N. Quan (2015). "Interleukin 1 type 1 receptor restore:
825 a genetic mouse model for studying interleukin 1 receptor-mediated effects in specific cell types." J
826 Neurosci **35**(7): 2860-2870.
827 Maes, M., A. H. Lin, L. Delmeire, A. Van Gastel, G. Kenis, R. De Jongh and E. Bosmans (1999). "Elevated
828 serum interleukin-6 (IL-6) and IL-6 receptor concentrations in posttraumatic stress disorder following
829 accidental man-made traumatic events." Biol Psychiatry **45**(7): 833-839.
830 Maes, M., C. Song and R. Yirmiya (2012). "Targeting IL-1 in depression." Expert Opin Ther Targets **16**(11):
831 1097-1112.
832 Marin, M. F., C. Lord, J. Andrews, R. P. Juster, S. Sindi, G. Arsenault-Lapierre, A. J. Fiocco and S. J. Lupien
833 (2011). "Chronic stress, cognitive functioning and mental health." Neurobiol Learn Mem **96**(4): 583-595.
834 McClung, C. A., P. G. Ulery, L. I. Perrotti, V. Zachariou, O. Berton and E. J. Nestler (2004). "DeltaFosB: a
835 molecular switch for long-term adaptation in the brain." Brain Res Mol Brain Res **132**(2): 146-154.
836 McKim, D. B., A. Niraula, A. J. Tarr, E. S. Wohleb and J. F. Sheridan (2016). "Neuroinflammatory Dynamics
837 Underlie Memory Impairments after Repeated Social Defeat." **36**(9): 2590-2604.
838 McKim, D. B., J. M. Patterson, E. S. Wohleb, B. L. Jarrett, B. F. Reader, J. P. Godbout and J. F. Sheridan
839 (2015). "Sympathetic Release of Splenic Monocytes Promotes Recurring Anxiety Following Repeated
840 Social Defeat." Biol Psychiatry.
841 McKim, D. B., M. D. Weber, A. Niraula, C. M. Sawicki, X. Liu, B. L. Jarrett, K. Ramirez-Chan, Y. Wang, R. M.
842 Roeth, A. D. Sucaldito, C. G. Sobol, N. Quan, J. F. Sheridan and J. P. Godbout (2017). "Microglial
843 recruitment of IL-1beta-producing monocytes to brain endothelium causes stress-induced anxiety." Mol
844 Psychiatry.
845 Menard, C., M. L. Pfau, G. E. Hodes, V. Kana, V. X. Wang, S. Bouchard, A. Takahashi, M. E. Flanigan, H.
846 Aleyasin, K. B. LeClair, W. G. Janssen, B. Labonte, E. M. Parise, Z. S. Lorsch, S. A. Golden, M. Heshmati, C.
847 A. Tamminga, G. Turecki, M. Campbell, Z. A. Fayad, C. Y. Tang, M. Merad and S. J. Russo (2017). "Social
848 Stress Induces Neurovascular Pathology Promoting Depression." Nature Neuroscience **20**.
849 Mendez-Ferrer, S., M. Battista and P. S. Frenette (2010). "Cooperation of beta(2)- and beta(3)-
850 adrenergic receptors in hematopoietic progenitor cell mobilization." Ann N Y Acad Sci **1192**: 139-144.
851 Miller, G. E., E. Chen, J. Sze, T. Marin, J. M. Arevalo, R. Doll, R. Ma and S. W. Cole (2008). "A functional
852 genomic fingerprint of chronic stress in humans: blunted glucocorticoid and increased NF-kappaB
853 signaling." Biol Psychiatry **64**(4): 266-272.
854 Miller, G. E., S. Cohen and A. K. Ritchey (2002). "Chronic psychological stress and the regulation of pro-
855 inflammatory cytokines: a glucocorticoid-resistance model." Health Psychol **21**(6): 531-541.
856 Miller, G. E., M. L. Murphy, R. Cashman, R. Ma, J. Ma, J. M. Arevalo, M. S. Kobor and S. W. Cole (2014).
857 "Greater inflammatory activity and blunted glucocorticoid signaling in monocytes of chronically stressed
858 caregivers." Brain Behav Immun **41**: 191-199.
859 Pace, T. W., T. C. Mletzko, O. Alagbe, D. L. Musselman, C. B. Nemeroff, A. H. Miller and C. M. Heim
860 (2006). "Increased stress-induced inflammatory responses in male patients with major depression and
861 increased early life stress." Am J Psychiatry **163**(9): 1630-1633.
862 Pasquali, R. (2012). "The hypothalamic-pituitary-adrenal axis and sex hormones in chronic stress and
863 obesity: pathophysiological and clinical aspects." Ann N Y Acad Sci **1264**: 20-35.

Perrotti, L. I., Y. Hadeishi, P. G. Ulery, M. Barrot, L. Monteggia, R. S. Duman and E. J. Nestler (2004). "Induction of deltaFosB in reward-related brain structures after chronic stress." J Neurosci **24**(47): 10594-10602.

Pierce, H., D. Zhang, C. Magnon, D. Lucas, J. R. Christin, M. Huggins, G. J. Schwartz and P. S. Frenette (2017). "Cholinergic Signals from the CNS Regulate G-CSF-Mediated HSC Mobilization from Bone Marrow via a Glucocorticoid Signaling Relay." Cell Stem Cell **20**(5): 648-658.e644.

Powell, N. D., E. K. Sloan, M. T. Bailey, J. M. Arevalo, G. E. Miller, E. Chen, M. S. Kobor, B. F. Reader, J. F. Sheridan and S. W. Cole (2013). "Social stress up-regulates inflammatory gene expression in the leukocyte transcriptome via beta-adrenergic induction of myelopoiesis." Proc Natl Acad Sci U S A **110**(41): 16574-16579.

Quan, N., R. Avitsur, J. L. Stark, L. He, W. Lai, F. Dhabhar and J. F. Sheridan (2003). "Molecular mechanisms of glucocorticoid resistance in splenocytes of socially stressed male mice." J Neuroimmunol **137**(1-2): 51-58.

Quan, N., R. Avitsur, J. L. Stark, L. He, M. Shah, M. Caligiuri, D. A. Padgett, P. T. Marucha and J. F. Sheridan (2001). "Social stress increases the susceptibility to endotoxic shock." J Neuroimmunol **115**(1-2): 36-45.

Ramirez, K., A. Niraula and J. F. Sheridan (2016). "GABAergic modulation with classical benzodiazepines prevent stress-induced neuro-immune dysregulation and behavioral alterations." Brain Behav Immun **51**: 154-168.

Reader, B. F., B. L. Jarrett, D. B. McKim, E. S. Wohleb, J. P. Godbout and J. F. Sheridan (2015). "Peripheral and central effects of repeated social defeat stress: Monocyte trafficking, microglial activation, and anxiety." Neuroscience.

Riddell, N. E., V. E. Burns, G. R. Wallace, K. M. Edwards, M. Drayson, L. S. Redwine, S. Hong, J. C. Bui, J. C. Fischer, P. J. Mills and J. A. Bosch (2015). "Progenitor cells are mobilized by acute psychological stress but not beta-adrenergic receptor agonist infusion." Brain Behav Immun **49**: 49-53.

Sapolsky, R. M., L. M. Romero and A. U. Munck (2000). "How do glucocorticoids influence stress responses? Integrating permissive, suppressive, stimulatory, and preparative actions." Endocr Rev **21**(1): 55-89.

Sawicki, C., D. McKim, E. Wohleb, B. Jarrett, B. Reader, D. Norden, J. Godbout and J. Sheridan (2014). "Social defeat promotes a reactive endothelium in a brain region-dependent manner with increased expression of key adhesion molecules, selectins and chemokines associated with the recruitment of myeloid cells to the brain." Neuroscience.

Smoak, K. A. and J. A. Cidlowski (2004). "Mechanisms of glucocorticoid receptor signaling during inflammation." Mech Ageing Dev **125**(10-11): 697-706.

Sorrells, S. F., J. R. Caso, C. D. Munhoz and R. M. Sapolsky (2009). "The stressed CNS: when glucocorticoids aggravate inflammation." Neuron **64**(1): 33-39.

Stark, J. L., R. Avitsur, D. A. Padgett, K. A. Campbell, F. M. Beck and J. F. Sheridan (2001). "Social stress induces glucocorticoid resistance in macrophages." Am J Physiol Regul Integr Comp Physiol **280**(6): R1799-1805.

Torres-Platas, S. G., C. Cruceanu, G. G. Chen, G. Turecki and N. Mechawar (2014). "Evidence for increased microglial priming and macrophage recruitment in the dorsal anterior cingulate white matter of depressed suicides." Brain Behav Immun.

Walker, B. R. (2007). "Glucocorticoids and cardiovascular disease." Eur J Endocrinol **157**(5): 545-559.

Weber, M. D., J. P. Godbout and J. F. Sheridan (2017). "Repeated Social Defeat, Neuroinflammation, and Behavior: Monocytes Carry the Signal." Neuropsychopharmacology **42**(1): 46-61.

Wohleb, E. S., A. M. Fenn, A. M. Pacenta, N. D. Powell, J. F. Sheridan and J. P. Godbout (2012). "Peripheral innate immune challenge exaggerated microglia activation, increased the number of

911 inflammatory CNS macrophages, and prolonged social withdrawal in socially defeated mice."
912 Psychoneuroendocrinology **37**(9): 1491-1505.
913 Wohleb, E. S., M. L. Hanke, A. W. Corona, N. D. Powell, L. M. Stiner, M. T. Bailey, R. J. Nelson, J. P.
914 Godbout and J. F. Sheridan (2011). "β-Adrenergic receptor antagonism prevents anxiety-like behavior
915 and microglial reactivity induced by repeated social defeat." J Neurosci **31**(17): 6277-6288.
916 Wohleb, E. S., D. B. McKim, D. T. Shea, N. D. Powell, A. J. Tarr, J. F. Sheridan and J. P. Godbout (2014).
917 "Re-establishment of Anxiety in Stress-Sensitized Mice Is Caused by Monocyte Trafficking from the
918 Spleen to the Brain." Biol Psychiatry.
919 Wohleb, E. S., D. B. McKim, J. F. Sheridan and J. P. Godbout (2014). "Monocyte trafficking to the brain
920 with stress and inflammation: a novel axis of immune-to-brain communication that influences mood and
921 behavior." Front Neurosci **8**: 447.
922 Wohleb, E. S., N. D. Powell, J. P. Godbout and J. F. Sheridan (2013). "Stress-induced recruitment of bone
923 marrow-derived monocytes to the brain promotes anxiety-like behavior." J Neurosci **33**(34): 13820-
924 13833.
925 Zhang, Y., K. Chen, S. A. Sloan, M. L. Bennett, A. R. Scholze, S. O'Keeffe, H. P. Phatnani and P. Guarnieri
926 (2014). "An RNA-sequencing transcriptome and splicing database of glia, neurons, and vascular cells of
927 the cerebral cortex." **34**(36): 11929-11947.
928 Zhou, D., A. W. Kusnecov, M. R. Shurin, M. DePaoli and B. S. Rabin (1993). "Exposure to physical and
929 psychological stressors elevates plasma interleukin 6: relationship to the activation of hypothalamic-
930 pituitary-adrenal axis." Endocrinology **133**(6): 2523-2530.

931

Figure 1

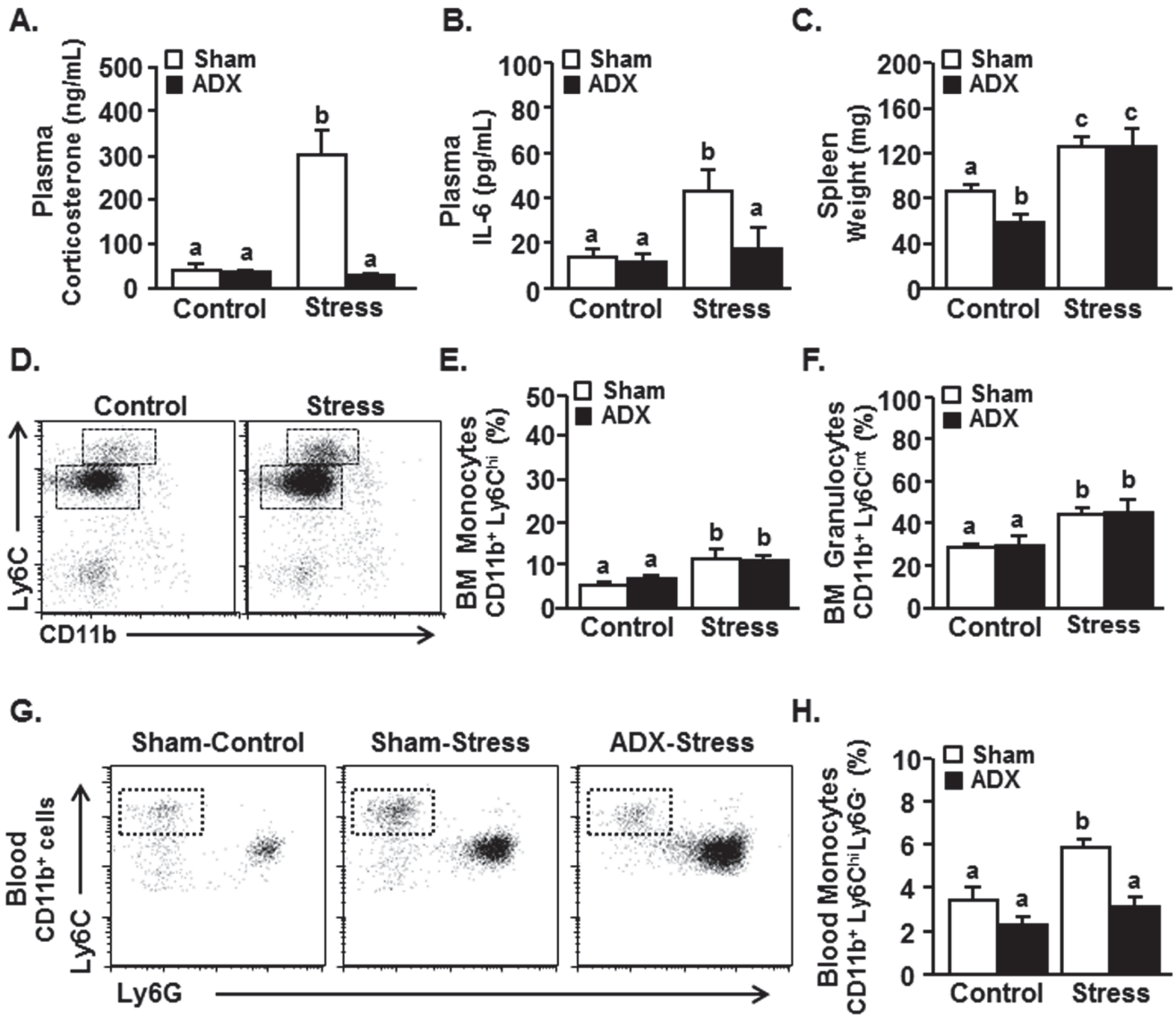

Figure 2

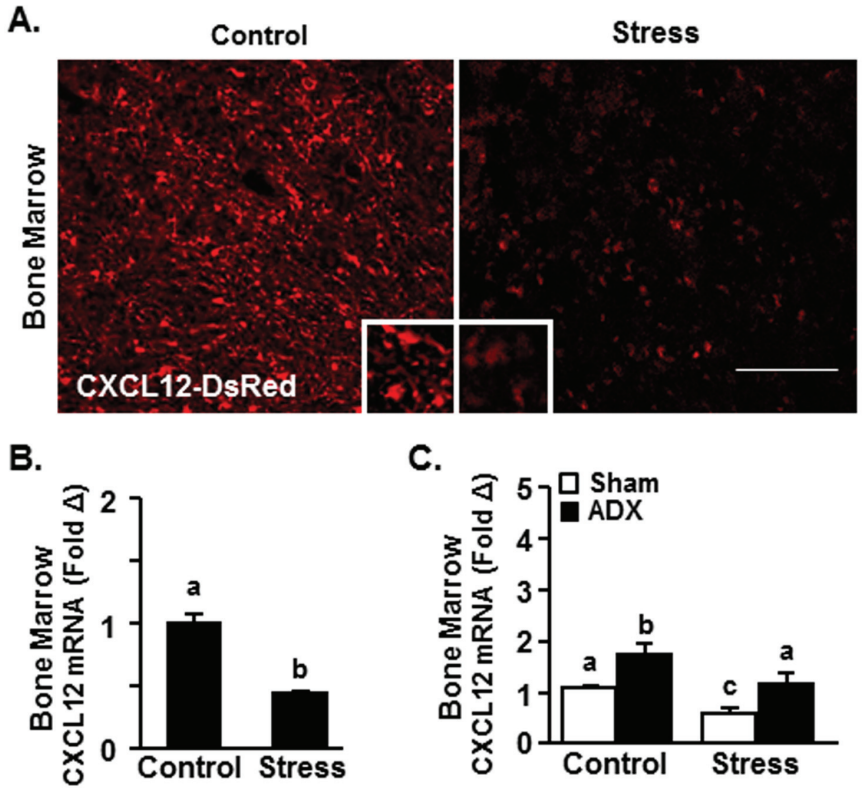

Figure 3

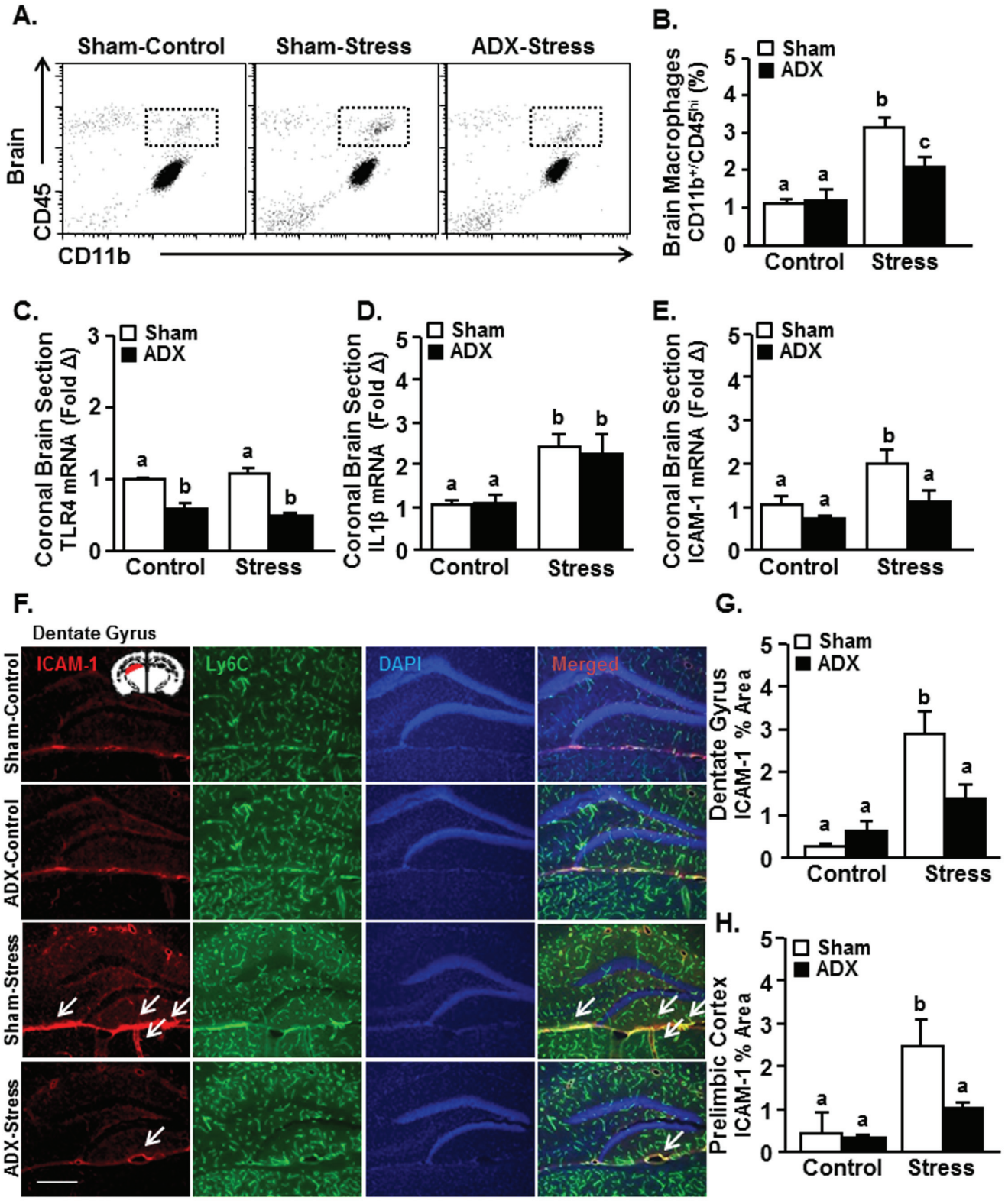

Figure 4

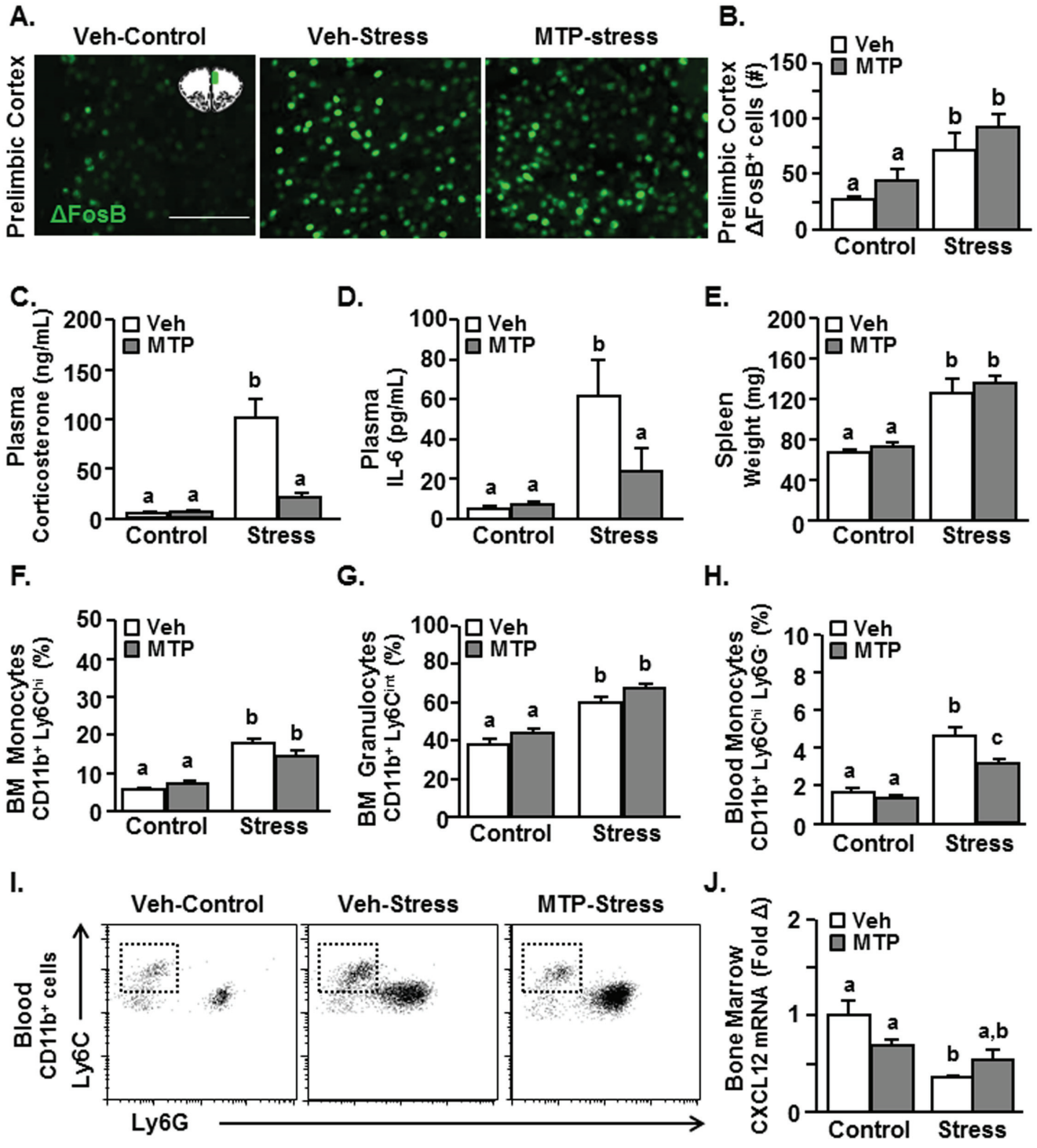

Figure 5

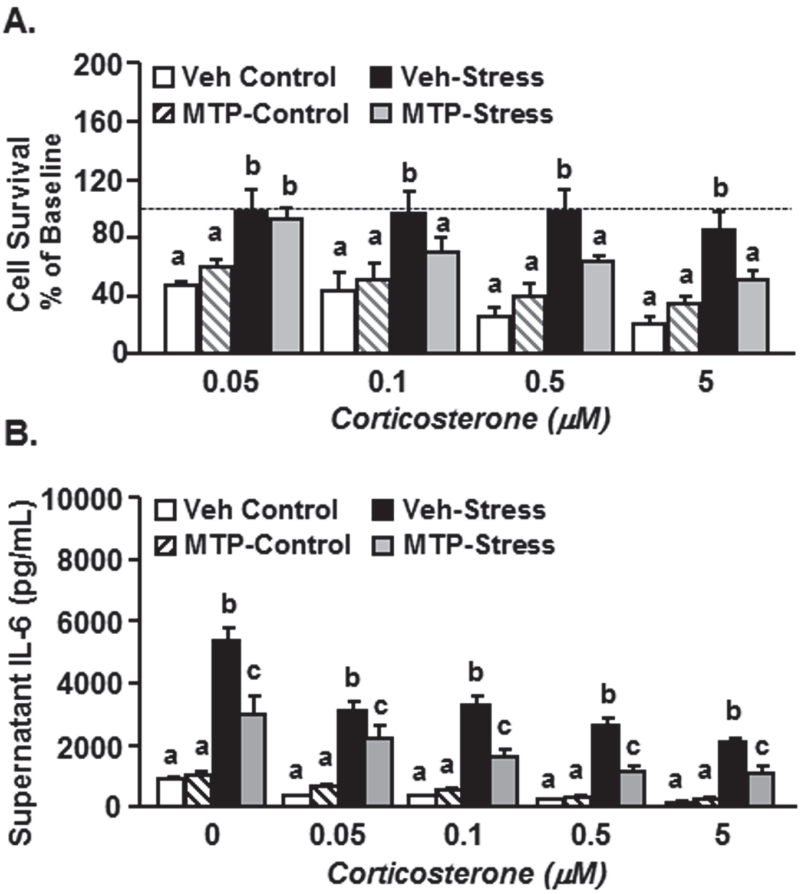

Figure 6

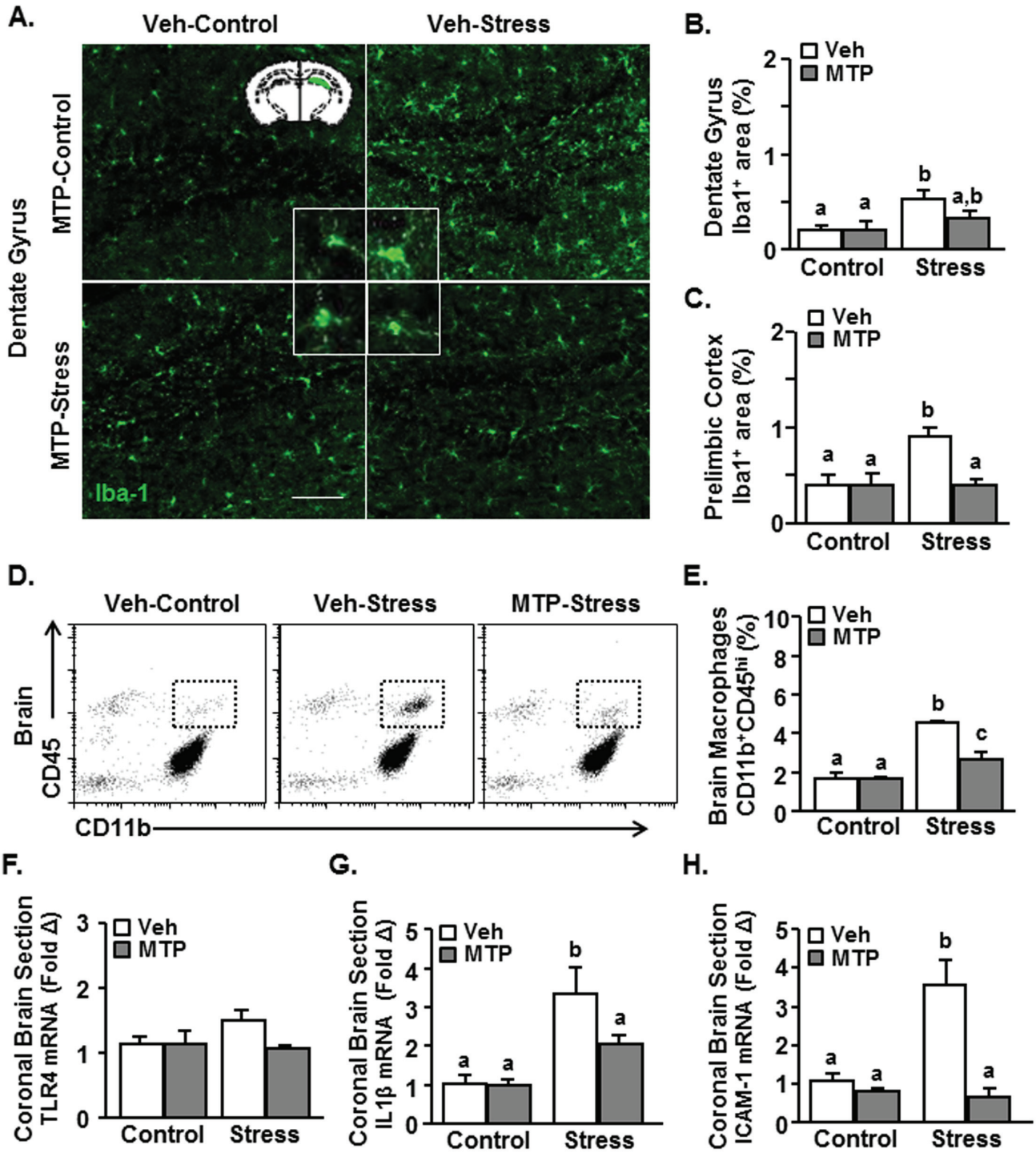

Figure 7